J. Phys.: Condens. Matter 7 (1995) 9369–9384. Printed in the UK

The stability of satellite faces on modulated crystals

M A Verheijen, C J M van den Hoogenhof, L J P Vogels and H Meekes

RIM Laboratory of Solid State Chemistry, Faculty of Science, University of Nijmegen, Toernooiveld, 6525 ED Nijmegen, The Netherlands

Received 2 August 1995

Abstract. Sphere growth experiments have been performed on a series of distorted β-K_2SO_4-type structures, all having a modulated crystal structure. An inventory of all satellite forms occurring was made. The stabilities of these forms were found to be clearly dependent on the length of the modulation wave vector. The results were compared with a connected net analysis and calculations on surface energies in a (1 + 1)-dimensional modulated crystal model. A qualitatively good agreement between experiments and theory was found. The selection rules of the superspace group were shown to be relevant.

1. Introduction

The crystal lattice of non-modulated crystals can be described by three independent periodicities indicated by the vectors a_1, a_2 and a_3. In modulated crystals at least one extra periodic distortion is present. In reciprocal space the periodic distortion is characterized by the modulation wave vector $q = \alpha a_1^* + \beta a_2^* + \gamma a_3^*$. In commensurately modulated structures these modulation wave parameters all have rational values. In that case a different unit cell can be defined that describes the lattice of the modulated crystal with—again—three vectors, resulting in a so-called superstructure. In incommensurately modulated crystal at least one of the parameters α, β and γ has an irrational value. The structure of the latter type of crystal has no translational symmetry in three dimensions. Nevertheless, the x-ray diffraction pattern, and thus the structure, can be described on a four-dimensional $\mathbb{Z}$-module in reciprocal space.

Strikingly, the presence of an extra periodicity in the crystal lattice has been observed on the habit of incommensurately modulated crystals. Most crystals are bound by macroscopic, flat faces. For non-modulated crystals these faces can be labelled with three indices (*hkl*), defining the reciprocal-lattice vectors $\boldsymbol{H}_{hkl} = h\boldsymbol{a}_1^* + k\boldsymbol{a}_2^* + l\boldsymbol{a}_3^*$ oriented perpendicularly to these faces. On the habit of modulated crystals, faces have been observed that have to be labelled using a fourth index m, referring to the modulation wave vector $\boldsymbol{q}$. These faces with $m \neq 0$ are called satellite faces. They are thus perpendicular to the reciprocal-lattice vector $\boldsymbol{H}_{hklm} = h\boldsymbol{a}_1^* + k\boldsymbol{a}_2^* + l\boldsymbol{a}_3^* + m\boldsymbol{q}$. Known examples of crystals displaying satellite faces are Rb_2ZnBr_4 and Rb_2ZnCl_4 [1, 2], calaverite ($Au_{1-x}Ag_xTe_2$) [3, 4] and $((CH_3)_4N)_2ZnCl_{4-x}Br_x$ (with $0 \leqslant x \leqslant 4$) [5, 6, 7, 8, 9].

For non-modulated crystals theories have been developed to explain and predict the stability of the crystal faces and the overall morphology [10]. A simplified model for the crystal faces can be obtained by cutting the crystal with a plane (*hkl*) perpendicular to the reciprocal-lattice vector $\boldsymbol{H}_{hkl}$. Concerning the stability of a face (*hkl*) two parameters are important. First, within a layer of thickness d_{hkl} a connected net of bonds between

0953-8984/95/499369+16$19.50

the growth units has to be present. Second, the stability of the face is dependent on the surface free energy, i.e. the total energy per unit area that is required to create the surface by breaking bonds. This model can be used to describe layer-by-layer crystal growth and predict the crystal morphology.

Because of lattice periodicity a connected net can be treated as a periodic repetition of F-slice cells with thickness d_{hkl} and surface (mesh) area M_{hkl}, the volume of the F-slice cell being equal to that of the crystallographic unit cell [10]. In order to check the connectedness and calculate the sum of broken-bond energies therefore only one F-slice cell needs to be considered. However, for incommensurately modulated crystals it is not always possible to define an F-slice cell that is periodically repeated on a face because of the breaking of the lattice periodicity due to the modulation. This would imply that for these kinds of face the entire surface has to be considered in order to calculate (average) surface free energies. Furthermore, these calculations would become rather involved because of the complicated surface structure.

In order to account for these problems Bennema *et al* and Kremers *et al* developed a theory that is able to explain the occurrence and stability of satellite faces [11, 12, 13]. In [9] and [10] the case of a modulated one-dimensional crystal was treated. This crystal was embedded in a (1 + 1)-dimensional superspace, where it has full translational symmetry. The description of modulated crystals in terms of a superspace embedding was introduced by de Wolff, Janner and Janssen [14, 15, 16, 17]. The physical (one-dimensional) space is then a section of the superspace. In [9] and [10] the chemical bonds are constructed parallel to the physical space. The phase of the modulation wave runs along the internal axis, i.e. perpendicular to the physical space, called external space. As in each phase the atoms are connected to each other by bonds, a bond density is created in superspace. As the positions of the atoms are modulated, a continuous range of bond lengths is obtained for an incommensurate value of the modulation wave parameter. When this crystal is cut by a grid of lines (hm), it was shown that for most faces only a fraction of all possible bonds are cut. This is called the principle of selective cuts. It will therefore be possible to find a phase of the modulation for which the surface free energy is lower than that of the same face for the non-modulated crystal. The principle of selective cuts thus introduces the stabilization of satellite faces.

Subsequently, surface free-energy calculations were performed for the equilibrium morphology of the one-dimensional modulated crystal as a function of α in $q = \alpha a^*$. The results are reproduced in figure 1 for a selected set of crystallographic planes. Plotted is the relative surface free energy (ξ/ξ_{max}) as a function of α. Here, $\xi/\xi_{max} = 1.00$ represents the surface free energy of the forms in the non-modulated crystal. It can clearly be seen that the satellite faces are indeed stabilized by the presence of a modulation. Their stability is shown to be strongly dependent on the value of α. As a result, the order in stability of the faces also changes noticeably with α. Also visible in this figure is a mirror symmetry line at $\alpha = 0.5$. This is present because for each modulation two descriptions are possible, giving the same displacements at the positions of the atoms, but different ones between the atoms, thus describing essentially the same crystal. These two modulations are related by: $q' = a^* - q$. Thus, a face (hm) for a certain value of α is equivalent to the $((h + m)\overline{m})$ face for $\alpha' = 1 - \alpha$.

The theory was later extended to modulated three-dimensional crystals embedded in a (3 + 1)-dimensional superspace [13]. It was shown there that the (3 + 1)-dimensional embedding can be described by a set of (1 + 1)-dimensional embeddings for the different modulated bond chains of the connected nets. This implies that the concepts and results of the (1 + 1)-dimensional case are still relevant for modulated three-dimensional crystals.

The first aim of this paper is to investigate the validity of the above-mentioned theory by comparing it with experimental data on the stability of satellite faces on modulated crystals. In order to obtain these data a modulated crystal is needed that displays satellite faces and that shows a variation in length of the modulation wave vector as a function of, for example, temperature. The first compound that we studied was $((CH_3)_4N)_2ZnCl_{3.88}Br_{0.12}$. For this compound it is possible to study the morphology for only a limited range in the modulation wave parameter γ, i.e. γ varies from 1/3 to 0.42 within the observable temperature range. Still, very interesting results can be obtained, as will be discussed in section 4.1.

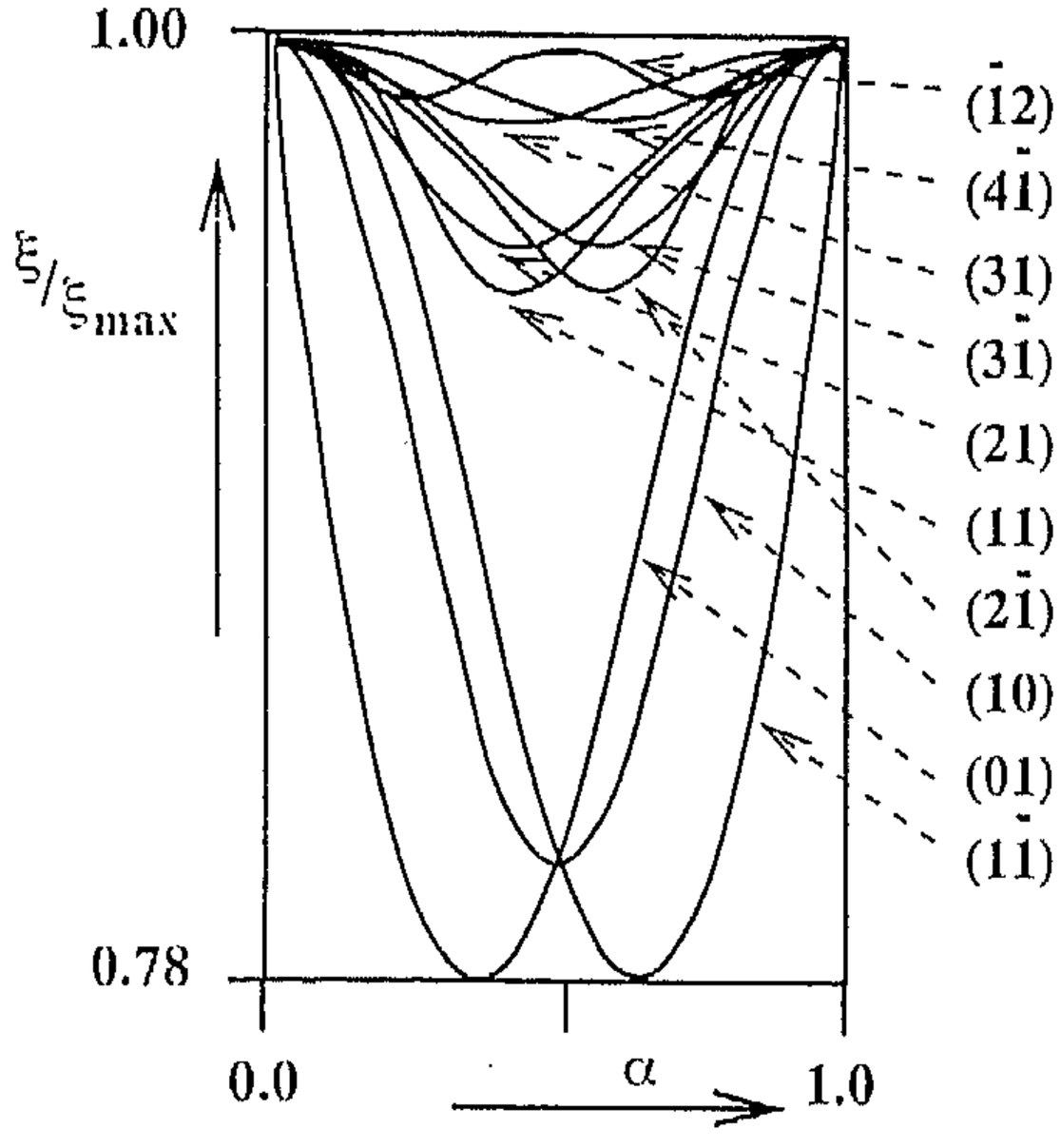

Figure 1. The relative surface free energy (ξ/ξ_{max}) as a function of the modulation wave parameter α. A representative set of faces has been plotted [12].

Because of the limited range in values of γ for the above-mentioned compound, we decided to consider several structurally related crystals as well. $((CH_3)_4N)_2ZnCl_{4-x}Br_x$ (with $0 \leqslant x \leqslant 4$) is a member of a group of distorted β-K_2SO_4-type structures. These kinds of structure have a sequence of phase transitions, the phases being either incommensurate structures or superstructures in which the atoms have coordinations that are analogous to those in β-K_2SO_4. The general chemical formula of these compounds is A_2BX_4, where B and X represent metal and halogen atoms respectively, while A can either represent metal ions such as Rb or positively charged groups such as $(CH_3)_4N$ (tma: tetramethyl ammonium). The modulation wave vector is parallel to c^* for all the compounds studied in our experiments. The incommensurate and commensurate phases can all be considered as one modulated phase with superspace symmetry group $Pcmn(00\gamma)(1s\bar{1})$ and varying modulation wave parameter γ [18, 19]. The three-dimensional space groups that are the symmetry groups (of the superstructures) in the commensurate phases are subgroups of the superspace group $Pcmn(00\gamma)(1s1)$. Using crystals of a series of A_2BX_4 compounds we were able to study the morphology for a large range of γ, while the average crystal structures of the different compounds were all isostructural. The results of these experiments are presented in section 4.2.

Because of the relatively low stability of most of the satellite faces in comparison to that of the main faces, all growth experiments were performed on spherical crystals. In this way all possible crystal faces get an equal chance to develop on the growth form.

Although in the theoretical modulated crystal model the (3 + 1)-dimensional embedding can be described by a set of (1 + 1)-dimensional embeddings, the results for the (1 + 1)-dimensional crystal as presented in figure 1 cannot be compared directly with the experimental results. A modulated bond chain with bond vector $\boldsymbol{b} = (b_1, b_2, b_3)$ is

in the (3 + 1)-dimensional superspace embedded in a two-dimensional plane spanned by $b_s = (b, 0)$ and $a_{4s} = (0, a_4)$. Therefore experimentally observed faces $(hklm)$ can only be compared directly to faces (lm) of the (1 + 1)-dimensional crystal model when merely modulated bond vectors $b = (0, 0, b_3)$ are present in the crystal lattice. As in the A_2BX_4 compounds most of the bonds are not parallel to the direction of the modulation wave, this condition does not hold. Nevertheless, the phenomenon of a dependence of the stability of satellite faces on the magnitude of the modulation wave parameter is expected to have a general validity. Therefore, it is still interesting to qualitatively compare the experimental results with the (1 + 1)-dimensional theory, as will be done in section 4.

As was mentioned above, together with the surface free energy, the connectedness is also an important parameter for the stability of main faces. Therefore, the second aim of this paper is to study the importance of this parameter for the stability of satellite faces. In section 5 a study on the connectedness of satellite forms will be presented. Subsequently, the results will be compared with the experimental data.

2. Experimental procedure

Crystals of A_2BX_4 compounds were grown from aqueous solutions either by slow evaporation of the solution at room temperature or by growth in a vessel as described in [20], which is based on a thermally induced convection. In this way single crystals of 0.1 to 1 cm^3 in size were obtained. Subsequently, these crystals were polished into spheres using a drilling device with a hollow spherical drill and water [8]. The spheres were put into a thermostated vessel containing a saturated solution. The vessel was closed thereafter, leaving, however, a small opening in order to allow for a slow continuous evaporation of the water. If desired, an undercooling was applied. All solutions contained several small crystals in order to keep the solution saturated on the one hand and on the other hand reduce the effective supersaturation which was initiated by an undercooling or evaporation of the solution. The growth parameters of the sphere growth experiments on the different A_2BX_4 compounds are summarized in table 1. It should be mentioned that around room temperature the solvability decreases with increasing temperature for solutions of $((CH_3)_4N)_2CoCl_4$.

Table 1. Growth temperature, growth time and supersaturation for the sphere growth experiments on the different A_2BX_4 compounds.

Compound		T_{growth} (°C)	Δt (h)	ΔT (°C)
$((CH_3)_4N)_2ZnCl_{3.88}Br_{0.12}$	(tmaZCB)	1–21	3	−0.1
$((CH_3)_4N)_2ZnCl_4$	(tmaZC)	8–22	3	−0.1
$((CH_3)_4N)_2CoCl_4$	(tmaCoC)	18–19	2–25	+ 2.0–+4.0
$((CH_3)_4N)_2MnCl_4$	(tmaMnC)	17–18	20–50	0 (slow evaporation)
$((CH_3)_4N)_2CuCl_4$	(tmaCuC)	24	20–150	0 (slow evaporation)
Rb_2ZnCl_4	(RbZC)	17–20	20–50	0 (slow evaporation)
Rb_2ZnBr_4	(RbZB)	17–20	4–10	0 (slow evaporation)

After growth, main faces as well as satellite faces could be observed on the spheres. Most of the latter faces appear as small spots on the growth form, surrounded by roughened parts. Because of the small size of these faces it is not possible to distinguish them from their surroundings using optical microscopy. Thus, they can only be detected using an optical goniometer. Some, however, appear as macroscopic faces. Using the goniometer the orientation of all faces was determined. The error in the position of the faces was

estimated to be $\pm 10'$, although larger deviations were found on spheres that had been allowed to grow for too short a period of time. The satellite reflections were all indexed in the superspace group $Pcmn(00\gamma)(1s\bar{1})$, as will be discussed in more detail in section 3. Reflections were only indexed when their orientation differed less than 1° from a theoretical one.

Besides presenting a list of observed satellite forms, we also consider the stability of these forms. One measure for the stability is the relative surface area. However, because of the small size of the satellite faces this criterion could not be used in our experiments. We therefore took the relative frequency of appearance ($\#_{rel}$) of a form as a measure for its stability. Here, $\#_{rel} = \#_{total}/(\#_{sph}\#_{sym})$, where $\#_{total}$ is the total number of faces of a certain form that were observed, $\#_{sph}$ the number of spheres studied and $\#_{sym}$ the number of symmetry-related faces of a certain form on the upper half of the sphere. Thus, for $\#_{rel}$ numbers ranging from 0 to 1 can be obtained.

The use of the relative frequency of appearance as a measure for the stability of faces is justified by the following. If one studies a series of crystals of a certain compound grown under the same conditions, one will observe that the relative surface area of each type of face will differ from crystal to crystal. This is caused by fluctuations of the growth parameters (e.g. convection), local defect densities, etc. For a large (i.e. stable) face this results in a certain range of surface areas. For less stable faces the average surface area is smaller. Thus, because of fluctuations in the growth process, for the latter faces it is frequently observed that they do not appear on the growth form. As a result the relative frequency of appearance will be lower than 100% for this kind of face. The less stable the face the more probable the situation that the face is not present on the growth form. This is the case for almost all satellite reflections on the spheres discussed in the present paper. Therefore, the relative frequency of appearance can be used as a measure for the stability of the satellite faces considered in our case.

3. Selection rules for satellite forms

In a layer-by-layer growth mechanism a crystal face (hkl) will grow with layers that are oriented perpendicularly to the reciprocal-lattice vector $\boldsymbol{H}_{hkl}$ and have a thickness equal to the distance between two adjacent equivalent lattice planes. According to the Bravais–Friedel–Donnay–Harker law [21, 22] a crystal form $\{hkl\}$ is more important for the crystal shape when this interlayer spacing is larger. This spacing is not equivalent for every form to the interplanar distance d_{hkl}, as the symmetry elements of the space group have to be taken into account. Consider, for example, a crystal structure containing a screw axis 2_1. For a face perpendicular to this screw axis the same surface configuration is repeated at $\frac{1}{2}d_{hkl}$. Therefore, this face is expected to grow with half-layers. Following the BFDH law the spacing d_{2h2k2l} is now a measure for the morphological importance (MI) of this face. It should be noted that the conditions for halving, trisecting and so on the thickness of the elementary growth layers are the same as those that apply to systematic extinctions in x-ray diffraction.

The question now arises of whether or not the BFDH law also holds in case of incommensurately modulated crystals. For these crystals, an interlayer spacing d_{hklm} can be defined for main as well as for satellite faces. However, other than for faces perpendicular to the modulation wave vector, no translational symmetry is present between the layers ($hklm$). Nevertheless, Kremers *et al* [13] showed that the average energy of the bonds cut by lattice planes ($hklm$) is the same for all lattice planes that are an integer number times d_{hklm} apart. Thus, for incommensurately modulated crystals 'equivalent' lattice planes can

also be defined. Therefore, one expects that the superspace group reflection conditions must be considered in order to obtain the smallest interlayer spacing.

As was mentioned in the introduction, the incommensurate and commensurate phases of the distorted β-K_2SO_4-type structures can each be considered as one modulated phase with symmetry group $Pcmn(00\gamma)(1s\bar{1})$ and varying modulation wave parameter γ. The reflection conditions for this superspace group are presented in table 2. All satellite faces that were observed in our experiments were indexed in this superspace group, taking its reflection conditions into account.

Table 2. Reflection conditions for the superspace group $Pcmn(00\gamma)(1s\bar{1})$ [16].

$hklm$	No conditions
$hk00$	$h + k$ even
$h0lm$	m even
$0klm$	l even

For the commensurately modulated crystal structures one could also choose to index the satellite faces according to the reflection conditions of the superstructures. For a structure, with $q = (r/s)a_3^*$ with r, s relatively prime integers, the face (h, k, l, m) will become $(h, k, sl + rm)$ in the superstructure notation. Application of the relating selection rules for some faces results in an altered restriction to the interlayer spacing, i.e. some of the superspace reflection conditions do not hold for certain superstructure symmetries. Where faces are involved that were observed in our experiments, this phenomenon will be discussed in more detail in the next section.

The choice to index the observed satellite faces in the superspace description for the commensurately modulated structures also is supported by experimental results; the point group of the incommensurately modulated phases is isomorphous to *mmm*, whereas the commensurately modulated phases generally have lower point group symmetries. Nevertheless, for all phases the faces $(\pm h \pm k \pm(l + m))$, which are symmetry equivalent as regards the point group symmetry *mmm*, were considered to belong to the same form $\{hklm\}$. This is justified by the fact that no significant difference in stability was observed for the different $(\pm h \pm k \pm(l + m))$ faces—neither in our work nor in the experiments of Dam and Janner [6].

4. Sphere growth experiments

4.1. Sphere growth experiments on $((CH_3)_4N)_2ZnCl_{3.88}Br_{0.12}$ crystals as a function of temperature

In table 3 the different crystal structures and the corresponding values for the modulation wave parameter as a function of temperature are given for $((CH_3)_4N)_2ZnCl_{3.88}Br_{0.12}$ (tmaZCB) crystals. As is mentioned in the caption of table 3, the existence of phase IV was only derived from the (x, T)-phase diagram of $((CH_3)_4N)_2ZnCl_{4-x}Br_x$ in [23] and was never observed experimentally. Phase IV was omitted in the interpretation of our data, because in our experiments the same crystals were used as in the work of Vogels *et al* [8], for which a direct transition from phase III to V was observed.

In our experiments some ten spheres of these crystals were allowed to grow at ten different temperatures, ranging from 1.7 to 20.4 °C. On these spheres many satellite faces were observed. Those that occurred on spheres grown in phase II could be identified

Table 3. Crystal phases of $((CH_3)_4N)_2ZnCl_{3.88}Br_{0.12}$. γ is the modulation wave parameter.

Phase	V	IV†	III	II	I
Temperature (°C)	<4	<6	<11	<22	>22
System	Monoclinic	Incommensurate	Orthorhombic	Incommensurate	Orthorhombic
Symmetry	$P112_1/n$	$Pcmn(00\gamma)(1s\bar{1})$	$Pc2_1n$	$Pcmn(00\gamma)(1s\bar{1})$	$Pcmn$
γ	1/3	$2/5-\delta$	2/5	$0.40<\gamma<0.42$	—

† The existence of phase IV was derived from the (x, T)-phase diagram as presented by Colla [23]. Vogels *et al* report on a direct transition from phase III to phase V at 5 °C [8].

unambiguously. However, in the commensurately modulated phases for all faces more than one form {*hklm*} could be assigned to the same face. For example, in the case where $\gamma = 1/3$ the {2002} and {101$\bar{2}$} forms correspond to the same crystal face orientations. As only the latter form was observed in the incommensurate phase, this form was chosen to index the corresponding faces in the commensurate phases as well.

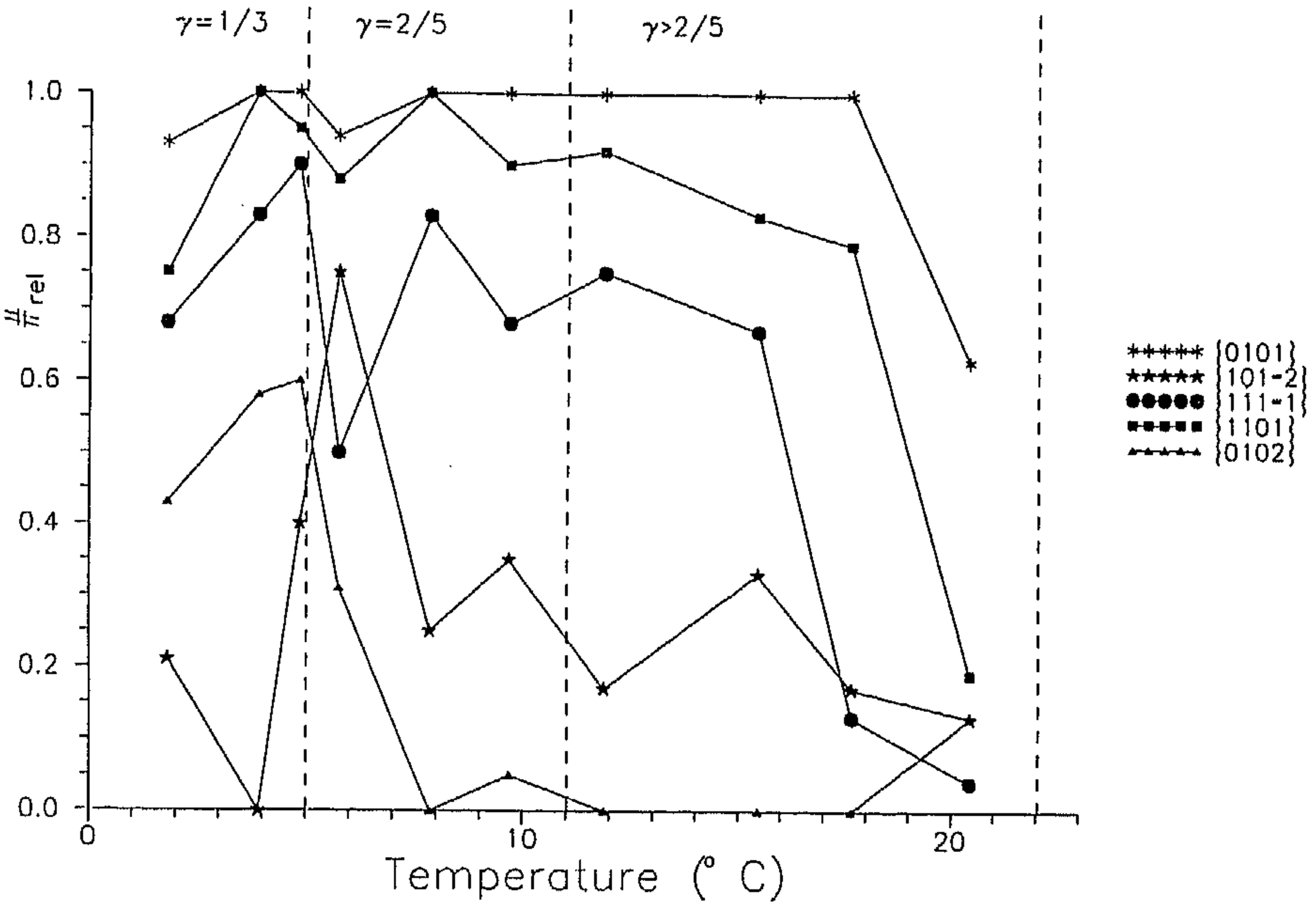

Figure 2. The relative frequency of occurrence ($\#_{rel}$) of five different satellite forms of tmaZCB as a function of temperature.

As a result, six different forms were observed more than once: the {0101}, {0102}, {101$\bar{2}$}, {1101}, {111$\bar{1}$} and {111$\bar{2}$} forms. The latter form was only observed twice. For the other forms the relative frequency of appearance as a function of temperature is given in figure 2. Clearly a difference in stability of the five satellite forms can be observed. The {0101} form is the most stable one at all temperatures. Its relative frequency of appearance is close to one for nearly the entire temperature range. Only at the highest temperature is a drop in the frequency observed. The latter phenomenon is present for the {101$\bar{2}$}, {1101} and {111$\bar{1}$} forms as well. Therefore, we conclude this to be a general feature due to the decrease in amplitude of the modulation close to the phase transition towards the para-phase (phase I). To understand this, one should keep in mind that the stability of satellite faces decreases with decreasing modulation amplitude [13].

Table 4. Frequencies of occurrence of satellite forms $\{hklm\}$ on spheres of several A_2BX_4 compounds. The relative frequency $\#_{rel}$ is given in brackets (in %). The forms $\{hklm\}$ and $\{hk(l+m)\overline{m}\}$ are presented together. Faces $(hkl\overline{2}l)$ and $(hk\overline{l}2l)$ belong to the same form.

	tmaZCB ($x = 0.12$)		tmaZCB ($x = 0.12$)		tmaZC		tmaCoC		tmaMnC		tmaCuC		RbZC	RbZB	
γ	1/3†		0.40†–0.42		0.40†–0.42		0.41		1/2†		0.674		0.69	0.706	
No of spheres	18		46		7		12		10		10		6	10	
0101	35	(97%)	88	(96%)	13	(92%)	23	(96%)	12	(60%)	15	(75%)	1	5	(25%)
$022\overline{2}$	‡		—		—		1	(4%)	‡	§	—		—	1	(5%)
0102	19	(53%)	7	(8%)	2	(14%)	—		1	(5%)	—		—	—	
$012\overline{2}$	—		—		—		—			§	2	(10%)	—	—	
0301	—		—		—		—		2	(10%)	1	(5%)	—	—	
$062\overline{2}$	—‡		—		—		3	(13%)	‡	§	1	(5%)	—	—	
0304	—		—		—		—		4	(20%)	1	(5%)	—	—	
$034\overline{4}$	—		—		—		—			§	1	(5%)	—	—	
$101\overline{2}$	7	(19%)	31	(34%)	6	(38%)	10	(42%)		{200}	6	(30%)	—	4	(20%)
1101	64	(89%)	159	(86%)	24	(86%)	12	(25%)	6	(15%)	8	(20%)	1	10	(25%)
$111\overline{1}$	52	(72%)	110	(60%)	16	(57%)	10	(21%)		§	28	(70%)		21	(53%)
1102			—		—		2	(4%)		{111}	1	(3%)	—	—	
$112\overline{2}$	—		—		—		—			§	1	(3%)	2	4	(10%)
$111\overline{2}$			3	(2%)	—		5	(10%)		{110}	1	(3%)	—	9	(23%)
$11\overline{1}4$			—		—		4	(8%)		{111}	—		—	—	
$113\overline{4}$	—		—		—		1	(2%)		§	—		—	—	
$112\overline{4}$			—		—		—			{110}	1	(3%)	—	4	(10%)

$200\bar{2}$	‡	—‡	—‡	2	(8%)		{201}	—		—	—	
$202\bar{2}$	—‡	—‡	—‡	1	(4%)		§	—		5	—	
2201	—	—	—	2	(4%)	8	(20%)	—		—	5	(13%)
$221\bar{1}$		—	—	4	(8%)		§	1	(3%)	—	1	(3%)
2211		—	—	2	(4%)	4	(10%)	1	(3%)	—	1	(3%)
$222\bar{1}$	—	—	—	1	(2%)		§	—		1	1	(3%)
$221\bar{2}$	—	—	—	2	(4%)		{110}	1	(3%)	1	9	(23%)
2212	—	—	—	—			{111}	—		—	—	
$223\bar{2}$	—	—	—	—			§	1	(3%)	—	3	(8%)
$221\bar{3}$		—	—	5	(10%)	8	(20%)	1	(3%)	1	2	(5%)
$222\bar{3}$	—	—	—	—			§	—		—	—	
2233	—	—	—	—		3	(8%)	—		—	—	
$226\bar{3}$	—	—	—	—			§	—		—	—	
4002	—‡	—‡	—‡	1	(4%)	3	(15%)	—		2	—	
$402\bar{2}$	‡	—‡	—‡	2	(8%)		§	2	(10%)	—	—	

† These structures are commensurately modulated.

‡ Double layers are allowed when indexing is done for the (commensurate) superstructure.

§ For tmaMnC the $\{hklm\}$ and $\{hk(l+m)\overline{m}\}$ forms have identical orientations.

In figure 2 the phase transition from phase V to III is indicated by a dashed line. At this transition there is a discontinuous jump in the modulation wave parameter from 1/3 to 2/5. As the change in γ for the tmaZCB crystals is largest at this temperature one would expect the largest change in stability of the different satellite forms at this phase transition. For the $\{10\bar{1}2\}$ and $\{0102\}$ forms a pronounced change in the relative frequency of appearance ($\#_{rel}$) can indeed be observed. The morphological importance of the $\{10\bar{1}2\}$ form significantly increases, whereas that of the $\{0102\}$ form decreases. Due to the large scatter in the data it is hard to draw any conclusions from the lines for the $\{1101\}$ and $\{111\bar{1}\}$ forms. The dependence of $\#_{rel}$ on γ is in any case less pronounced for the latter forms than it is for the former ones. In conclusion, the stability of (at least some of) the satellite forms is clearly dependent on the length of the modulation wave parameter. We will now first present the results of the sphere growth experiments on a series of A_2BX_4 compounds for which a larger range of γ was studied. Subsequently, all results will be compared to the theoretical results as shown in figure 1.

4.2. Sphere growth experiments on a series of A_2BX_4 compounds

Sphere growth experiments have been performed on seven different A_2BX_4 compounds. In table 4 the results of these studies are summarized. For each compound the frequency of occurrence of satellite forms as well as $\#_{rel}$ is given. Due to imperfections of the crystal surfaces it is possible that 'false reflections' are detected by the goniometer and thus are erroneously indexed as satellite reflections. To overcome this problem forms $\{hklm\}$ were only considered when they or their related $\{hk(l+m)\bar{m}\}$ forms were observed more than twice for one of the compounds. As was mentioned above, the indexing of the satellite forms was done in the superspace group $Pcmn(00\gamma)(1s1)$.

The results for tmaZCB that were presented in figure 2 are given in the second and third columns of table 4. Again, the change in stability of the $\{0102\}$ and $\{10\bar{1}2\}$ forms at the V ($\gamma = 1/3$) to III ($\gamma = 2/5$) phase transition is clearly visible. In the table a drop in the stability of the $\{111\bar{1}\}$ form also seems to be present going from phase V to III. However, this is not due to a stability dependence on γ, but on a dependence on the amplitude of the modulation vector as was discussed in the previous section.

Also for the six other A_2BX_4 compounds the observed satellite forms are presented. For RbZC, RbZB and tmaZC the existence of satellite faces has been reported before [1, 2, 4–7]. In contrast to the experimental results described by Janner *et al* [1] in which large satellite faces were observed on RbZC single crystals, in our studies no macroscopic satellite faces and hardly any satellite reflections were found on spheres of this compound. Only the $\{202\bar{2}\}$ form was observed more than twice. The low stability of satellite faces on RbZC spheres had already been reported by Dam and Janner [6]. In their experiments on RbZC they did not succeed in obtaining any satellite faces at all.

For tmaMnC the spheres were grown in the commensurately modulated phase, where $\gamma = 1/2$. As a result, the $\{hklm\}$ and $\{hk(l+m)\bar{m}\}$ forms have identical orientations. This is indicated by the '§' signs in the sixth double column. Furthermore, several satellite faces have the same orientation as main faces, e.g. the (1102) (satellite) face is identical to the (111) (main) face. Therefore, a face was only considered to be a satellite face when its orientation was not parallel to one of the main F faces as predicted by Vogels *et al* [24]. For all faces that did not fulfil this criterion the related main face is given in table 4.

As for tmaCuC the value for the modulation wave parameter was close to the commensurate value 2/3, for several faces an ambiguity in assignment was also present. For two reasons, however, we were still able to uniquely assign these satellite reflections

In table 4 six more sets of $\{hk0m\}/\{hkm\bar{m}\}$ forms are presented. However, due to the low stabilities of these forms it is not possible to draw any meaningful conclusions from these data. Despite their low stabilities it is still interesting to present the observation of these faces. The fact that they do show up on the growth form indicates that these faces are stable, though much less stable than the main faces. It shows that they are essentially different from any form $(hklm)$ that does not show up, as the former have an edge free energy that is essentially larger than zero.

The only other form in table 4 that allows for a comparison with the theoretical results is $\{10\bar{1}2\}$. As the curve of the $(\bar{1}2)$ face in figure 1 is symmetric around $\alpha = 1/2$ one would expect equal frequencies of occurrence for experiments for above and below 1/2. Indeed, the $\{10\bar{1}2\}$ form was observed for the entire range of γ and no significant differences between the stabilities above and below $\gamma = 1/2$ can be found. Whether a minimum in stability is present at $\gamma = 1/2$, as was predicted in figure 1, could not be determined, as the $\{10\bar{1}2\}$ form is identical to the $\{2000\}$ form for this value of the modulation wave parameter. Nevertheless, a decrease in stability for small and large values of γ for this face is indeed observed.

It is also interesting to directly compare different compounds that have the same value for γ. For $\gamma \approx 0.41$ three compounds have been studied; tmaZCB, tmaZC and tmaCoC. For tmaZCB and tmaZC the results are very similar. Apart from the occurrence of the $\{11\bar{1}2\}$ form on tmaZCB spheres, the same set of faces is found for these two compounds. Furthermore, the relative frequencies of occurrence are very similar for all forms. The spheres of tmaCoC show a slightly different morphology. The most important forms are the same as those on the other two compounds. However, $\#_{rel}$ is clearly different for the $\{1101\}$ and $\{111\bar{1}\}$ forms as was already mentioned above. Furthermore, the spheres of tmaCoC display a much larger number of satellite forms than do those of tmaZC and tmaZCB. The reason for the latter fact might be rather trivial: the spheres of tmaZC and tmaZCB were grown at a larger supersaturation than those of tmaCoC. This might have introduced kinetical roughening of the less stable satellite faces [10]. The difference between the stabilities of the $\{1101\}$ and $\{111\bar{1}\}$ forms cannot be explained by the influence of the supersaturation and will thus be due to the difference in growth units or to a difference in the modulation amplitude of these structures.

As was mentioned in section 3, for the commensurately modulated phases indexing can also be performed in the related superstructures. Application of the reflection conditions of these structures results in changed restrictions for some of the faces. For example, tmaZCB has the monoclinic structure $P112_1/n$ for $\gamma = 1/3$. The reflection conditions for this structure are: $hk0$: $h+k$ even; $00l$: l even. Thus, (1001), which is (101) in the monoclinic superstructure, is not forbidden, which is in contrast to the selection rules for the superspace group. All faces for which a doubling of the elementary growth layer is only allowed in the superstructure notation are indicated in table 4. Unfortunately, it cannot be concluded from this table whether the latter faces do indeed grow with double layers; a relatively higher stability indicating a doubled interlayer spacing d_{hklm} could not be observed for these faces.

In summary, for the most frequently observed satellite forms a clear dependence of their stability on the magnitude of the modulation wave parameter was observed. Strikingly, these dependences were qualitatively in good agreement with the predictions from the (1 + 1)-dimensional modulated crystal model. In order to allow for a more well founded comparison calculations concerning a (3 + 1)-dimensional embedding of the modulated A_2BX_4 compounds will be performed in the near future.

5. The connectedness of satellite forms

As was mentioned in the introduction, as well as the surface free energy, the connectedness is also an important parameter for the stability of a crystal face. In the previous section attention was focused on the comparison of the experimental results with the theoretically obtained surface free energies. Here, we will compare the experimental data with studies on the connectedness of the satellite forms.

The surface structure of the satellite faces was studied with the help of a computer program and graphics utilities. Our approach consisted of several stages. First, the crystal lattice had to be defined. The x-ray diffraction data for the average structure of tmaZC [25] were used to construct the unmodulated unit cell. Second, the tmaZC lattice was reduced to a crystal graph, in which the tma units and the ZC units were reduced to centres of gravity, being connected by lines representing bonds. A detailed description of the crystal graph and the set of bonds used is given in [24]. In our model the influence of the modulation on the position of the atoms was neglected. This is justifiable, as the maximal deviation from the average positions is only a few per cent of the average lattice parameters [26]. Next, a slice was cut parallel to a face $(hklm)$. The thickness of this slice was taken to be equal to the interlayer spacing d_{hklm}, corrected for the superspace selection rules. The building units and bonds within the slice were projected in a two-dimensional plot. In this way the connectedness of the slice could be checked visually. For all faces $(hklm)$ slices with thickness d_{hklm} were cut at ten different heights within one interlayer spacing d_{hklm}. For all satellite faces that had been observed in the experiments on the A_2BX_4 spheres the connectedness was thus studied for nine different values of the modulation wave parameter γ. It should be noted that in our model a change in γ does not result in changes in the crystal graph. Changes only occur in the orientations of the satellite faces and thus in the directions in which the slices are cut. The crystal graphs used consisted of at least 1000 unit cells.

The results of this study are presented in table 5. In order to be able to compare these results with the data in table 4, we assume that the results for tmaZC are representative for the whole set of A_2BX_4 compounds. This is justified, because in our model the unperturbed unit cell of tmaZC is used and this unit cell is very similar to those of the other A_2BX_4 compounds (see, for example, [27]). Furthermore, we assume that the modulation amplitude is also small for the other A_2BX_4 compounds. We think that this is justified as the relative frequencies of occurrence of the satellite forms are not significantly larger for the other compounds.

As can be seen in table 5 the connectivity of satellite forms depends on the value of the modulation wave parameter γ; the {1102} form, for example, is only connected for values up to 0.71. Table 5 shows that the most frequently observed satellite forms (i.e. {0101}, {0102}, $\{10\bar{1}\bar{2}\}$, {1101}, $\{11\bar{1}\bar{1}\}$ and $\{11\bar{1}\bar{2}\}$) are all connected for the entire range of γ. Moreover, many of the forms that were observed less frequently appear not to be connected. It can thus be concluded that the connectedness is an important criterion also for the stability of a satellite form.

However, one should keep several things in mind. First, in table 5 the connectedness is only given qualitatively. No data have been given on the (relative) strength of the connected nets. The {0102} form, for example, is connected for the entire range of γ, but the net is much weaker at higher values of γ than at lower values. This is also reflected in the observed frequency of appearance: the {0102} form was only observed in the case where $\gamma \leqslant 1/2$. For values of γ up to 0.91 the {2002} form has a surface that consists of large connected parts, separated by narrow strips in which no bonds are present, whereas this form

Table 5. The connectedness of the satellite faces that have been observed experimentally; c = connected, nc = not connected. The range of γ that is studied experimentally is 1/3–0.706.

γ	0.11	0.21	0.31	0.41	0.51	0.61	0.71	0.81	0.91
0101	c	c	c	c	c	c	c	c	c
$022\bar{2}$	nc	nc	nc	nc	c	nc	c	c	c
0102	c	c	c	c	c	c	c	c	c
$012\bar{2}$	c	c	c	c	c	c	c	c	c
0301	nc	nc	nc	nc	nc	nc	nc	nc	nc
$062\bar{2}$	nc	nc	nc	nc	nc	nc	nc	nc	nc
0304	nc	nc	nc	nc	nc	nc	nc	nc	nc
$034\bar{4}$	nc	nc	nc	nc	nc	nc	nc	nc	nc
$101\bar{2}$	c	c	c	c	c	c	c	c	c
1101	c	c	c	c	c	c	c	c	c
$111\bar{1}$	c	c	c	c	c	c	c	c	c
1102	c	c	c	c	c	c	c	nc	nc
$112\bar{2}$	nc	nc	c	c	c	c	c	c	c
$111\bar{2}$	c	c	c	c	c	c	c	c	c
$11\bar{1}4$	c	c	c	c	c	c	nc	nc	nc
$113\bar{4}$	nc	nc	nc	c	c	c	c	c	c
$112\bar{4}$	c	c	c	c	c	c	c	c	c
2002	c	c	c	nc	c	nc	nc	nc	nc
$202\bar{2}$	nc	nc	nc	nc	c	nc	c	c	c
$220\bar{1}$	c	nc	nc	nc	nc	nc	nc	nc	nc
2211	nc	nc	nc	nc	nc	nc	nc	nc	c
$221\bar{1}$	nc	nc	nc	nc	nc	nc	nc	nc	nc
$222\bar{1}$	nc	nc	nc	nc	nc	nc	nc	nc	nc
$221\bar{2}$	nc	nc	nc	nc	c	nc	nc	nc	nc
2212	nc	nc	nc	nc	c	nc	nc	nc	nc
$223\bar{2}$	nc	nc	nc	nc	c	nc	nc	nc	nc
$22\bar{1}3$	c	nc	nc	nc	nc	nc	nc	nc	nc
$222\bar{3}$	nc	nc	nc	nc	nc	nc	nc	nc	c
2233	nc	nc	nc	nc	nc	nc	nc	nc	nc
$226\bar{3}$	nc	nc	nc	nc	nc	nc	nc	nc	nc
4002	nc	nc	nc	nc	nc	nc	nc	nc	nc
$402\bar{2}$	nc	nc	nc	nc	nc	nc	nc	nc	nc

is reported to be connected only up to 0.31. A more quantitative approach for describing the strength of connected nets of satellite faces was described by Vogels *et al* [28]. In their study, the roughening temperature of a net is estimated from the ratio of weaker and stronger parts of the net. Still, this method can only be used for connected nets.

Second, because of the limited size of the crystal graph considered, the connectedness could only be checked for a limited surface area. Because of the lack of translational symmetry on the surface the possibility that nets that seem to be connected are not connected cannot be excluded.

Finally, the connectedness was studied using a limited set of bonds in the crystal graph. The addition of several (weaker) bonds to the crystal graph might introduce connectedness for some of the nets. For several of the nets, however, connectedness is not expected even

after the introduction of additional bonds. Still, some of these forms have been observed experimentally (e.g. the {0304} form).

Here, one should keep in mind that in our model a flat box is used to cut crystal faces. The actual surface structure, however, is still unknown and might show undulations. Moreover, the growth mechanism is unclear. Therefore, a quantitative analysis of our data is still impossible.

In summary, the connectedness of satellite forms clearly has a stabilizing effect on the presence of these forms on the growth form. However, forms that are not connected have also been observed experimentally.

6. Conclusions

Upon growth from aqueous solutions spherical crystals of distorted β-K_2SO_4-type structures displayed a large number of satellite faces. Indexing in the superspace group $Pcmn(00\gamma)(1s\bar{1})$ resulted in 29 different satellite forms. Nearly all forms were observed on more than one type of sphere. For the most frequently observed ones a very pronounced dependence of their stability on the length of the modulation wave vector was observed. The stability dependences of these forms (*hklm*) were qualitatively in rather good agreement with the predictions for forms (*hm*) resulting from the theory for modulated one-dimensional crystals of Bennema *et al* and Kremers *et al*. The application of superspace selection rules appeared to be relevant.

Furthermore, theoretical studies on the structure of satellite faces indicated that the connectedness of these faces is dependent on the length of the modulation wave vector. A comparison with the experimental results showed that the most stable satellite forms were all connected and that the stabilities of these forms increase when the strength of their connected nets increase. However, connectedness appeared not to be a strict requirement for satellite forms to be stable, because a considerable proportion of the observed forms were not connected. The latter forms, however, were the least stable ones.

Acknowledgments

We are very grateful to M Kremers and P Bennema for fruitful discussions. One of the authors, M A Verheijen, gratefully acknowledges the financial support of the Netherlands Organization for Scientific Research (NWO/SON).

References

[1] Janner A, Rasing T, Bennema P and van der Linden W H 1980 *Phys. Rev. Lett.* **45** 1700
[2] Dam B, Janner A, Bennema P, van der Linden W H and Rasing T 1983 *Phys. Rev. Lett.* **50** 849
[3] Dam B, Janner A and Donnay J D H 1985 *Phys. Rev. Lett.* **55** 2301
[4] Janner A and Dam B 1989 *Acta Crystallogr.* A **45** 115
[5] Dam B 1985 *Phys. Rev. Lett.* **55** 2806
[6] Dam B and Janner A 1986 *Acta Crystallogr.* B **42** 69
[7] Dam B and Bennema P 1987 *Acta Crystallogr.* B **43** 64
[8] Vogels L J P, Verheijen M A, Meekes H and Bennema P 1992 *J. Cryst. Growth* **121** 697
[9] Vogels L J P, Meekes H and de Boer J L 1994 *J. Phys.: Condens. Matter* **6** 8205
[10] Bennema P and van der Eerden J P 1987 *Morphology of Crystals* part A, ed I Sunagawa (Tokyo: Terra Scientific and Dordrecht: Reidel)
[11] Bennema P, Kremers M, Meekes H, Balzuweit K and Verheijen M A 1993 *Discuss. Faraday Soc.* **95** 2
[12] Kremers M, Meekes H, Bennema P, Balzuweit K and Verheijen M A 1994 *Phil. Mag.* B **69** 69

[13] Kremers M, Meekes H, Bennema P, Verheijen M A and van der Eerden J P 1995 *Acta Crystallogr.* A at press
[14] de Wolff P M 1974 *Acta Crystallogr.* A **30** 777
[15] Janner A and Janssen T 1977 *Phys. Rev.* B **15** 643
[16] de Wolff P M, Janssen T and Janner A 1983 *Acta Crystallogr.* A **37** 625
[17] Janner A, Janssen T and de Wolff P M 1983 *Acta Crystallogr.* A **39** 671
[18] Hogervorst A C R 1986 *PhD Thesis* Delft
[19] Janssen T 1986 *Ferroelectrics* **66** 203
[20] Arend H, Perret R, Wüest H and Kerkoc P 1986 *J. Cryst. Growth* **74** 321
[21] Friedel G 1907 *Bull. Soc. Fr. Minéral.* **30** 326
[22] Donnay G D H and Harker D 1937 *Am. Miner.* **22** 446
[23] Colla E L 1987 *PhD Thesis* Zürich
[24] Vogels L J P, Verheijen M A and Bennema P 1991 *J. Cryst. Growth* **110** 604
[25] Wiesner J R, Srivastava R C, Kennard C H L, Di Vaira M and Lingafelter E C 1966 *Acta Crystallogr.* **23** 565
[26] Madariaga G, Zuñiga F J, Pérez-Mato J M and Tello M J 1987 *Acta Crystallogr.* B **43** 356
[27] Perret R, Godefroy G and Arend H 1987 *Ferroelectrics* **73** 87
[28] Vogels L J P, Balzuweit K, Meekes H and Bennema P 1992 *J. Cryst. Growth* **116** 397